AJNR

Hyperostosis in meningiomas: MR findings in patients with recurrent meningioma of the sphenoid wings.

K Terstegge, W Schörner, H Henkes, N Heye, N Hosten and W R Lanksch

AJNR Am J Neuroradiol 1994, 15 (3) 555-560
http://www.ajnr.org/content/15/3/555

Hyperostosis in Meningiomas: MR Findings in Patients with Recurrent Meningioma of the Sphenoid Wings

K. Terstegge, W. Schörner, H. Henkes, N. Heye, N. Hosten, and W. R. Lanksch

PURPOSE: We used MR imaging to analyze retrospectively the pattern of hyperostosis occurring concomitantly with recurrent sphenoid wing meningiomas. **METHODS:** Bone involvement was compared in 12 corresponding CT and MR studies of 10 female patients with sphenoid wing meningiomas recurrence after earlier surgical treatment. Four of these had histologically confirmed meningiomatous infiltration of the bone. **RESULTS:** All patients had CT findings of localized hyperostosis of parts of the sphenoid wings. MR revealed inhomogenous areas of slightly increased signal intensity in hyperostotic bone on T2-, proton density- and T1-weighted sequences. In nine of 10 patients, segments of the hyperostotic bone showed different degrees of gadolinium enhancement. **CONCLUSIONS:** Because earlier studies have revealed high incidences of meningiomatous bone infiltration in sphenoid wing meningiomas, and because infiltration was confirmed in four of our patients, we postulate that the gadolinium enhancement in the area of hyperostosis may be related to meningiomatous bone infiltration.

Index terms: Sphenoid bone; Meninges, neoplasms; Brain neoplasms, magnetic resonance; Skull, abnormalities and anomalies

AJNR Am J Neuroradiol 15:555–560, Mar 1994

In some patients with intracranial meningiomas, localized hyperostosis of adjacent bone can be observed. The estimated incidence of this feature varies between 4.5% and 44% (1, 2). Some authors postulate that meningiomatous tumor infiltration of the bone is the cause of the hyperostosis (3–6). Others assume a hypertrophic bone reaction not dependent on tumor invasion, and have suggested that it may be caused by vascular hyperperfusion in the area of the meningioma, or other mechanisms (7–10). For sphenoid wing meningiomas, the incidence of hyperostosis reaches 90% and more (4, 6, 11–13). In all reported series of sphenoid wing meningiomas, histopathologic examinations revealed high incidences of meningiomatous infiltration of the affected bony tissue (4–6, 8, 11–13). Computed tomography (CT) is useful in the diagnosis of osseous changes in sphenoid wing meningiomas (6, 11). Although the intracranial features of meningiomas as demonstrated by magnetic resonance (MR) imaging have been studied extensively (14, 15), the MR characteristics of concomitant hyperostosis have received scant attention. The purpose of this study was to determine the MR characteristics of bony changes in sphenoid wing meningiomas in relation to the reported infiltrative behavior of the tumor.

Patients and Methods

We analyzed 12 corresponding CT and MR studies of 10 women with recurrence of sphenoid wing meningiomas. These were all the patients with a diagnosis of recurrent sphenoid wing meningiomas having undergone MR examination in our department before September 1992. Eight of them were between 42 and 55 years of age, one was 69, and one 80 (median 47.5 years). The patients had been referred for examination by different neurosurgical institutions; the intervals between the operation and the MR examination ranged from 1 to 8 years in eight patients, and was 17 and 22 years in the two oldest patients (patients

Received August 21, 1992; accepted pending revision October 21, revision received April 27, 1993.

From the Department of Radiology (K.T., W.S., N.Ho.), Institute of Neuropathology (N.He.), and Department of Neurosurgery (W.R.L.), Rudolf Virchow Hospital, Freie Universität Berlin; and Department of Radiology, Alfried Krupp Krankenhaus (H.H.), Essen, Germany.

Address reprint requests to K. Terstegge, MD, Department of Radiology, Rudolf Virchow University Hospital, Freie Universität Berlin, Augustenburger Platz 1, 13353 Berlin, Germany.

AJNR 15:555–560, Mar 1994 0195-6108/94/1503-0555

8 and 10; median 4.5 years). The diagnosis was proved by operation in all and the recurrence by repeat surgery in three patients. Four patients had "en plaque"-type sphenoid wing meningiomas (patients 1–4) and six others (patients 6–10) globoid or "en masse"-type sphenoid wing meningiomas. One patient (patient 8) had received adjuvant radiation therapy. A review of histopathologic samples revealed that decalcified hematoxylin-eosin sections of hyperostotic bone were still available for only four patients (patients 2, 3, 4, 10). All four samples showed massive infiltration of the bone, especially in the Haversian channels, by broad meningiomatous streaks.

MR was performed at 0.5 T on a medium-field body scanner. The protocols of axial tomography included a T2-weighted spin-echo sequence (1600/70/1 [repetition time/echo time/excitations], nine of 12 studies), a proton density–weighted spin-echo sequence (1600/30/1, nine of 12 studies) and T1-weighted gradient-echo sequences (315/14/1, 90° flip angle) before and after (11 of 12 studies) application of 0.1 mmol/kg gadopentetate dimeglumine. Coronal T1-weighted sections were obtained without contrast medium and after administration of contrast medium (11 of 12 studies). The interval between the CT and the MR examinations was less than 3 months. All CT studies included axial tomograms in the gantry position parallel to the orbitomeatal plane, a contrast-enhanced series, and images at bone window settings, the latter predominantly in high resolution technique. In individual cases additional primary tomograms in infraorbitomeatal and/or coronal planes had been obtained. The planes of the CT scans and MR axial tomograms varied, and the differences were carefully considered on evaluation.

The presence and location of hyperostosis (broadening of bone, increased density, and structural changes) were evaluated on CT scans at bone window level. The CT density of the hyperostotic mass was rated relative to contralateral normal bone. The structure of this mass was classified as plaque-shaped, coarse-trabecular, or normal. The tabular architecture in the same area was rated as distinguishable or not distinguishable.

The signal intensity of corresponding anatomical structures was rated in MR examinations, relative to normal bone of the contralateral skull (mildly, moderately, or markedly increased). The distinguishability of tabular bone architecture was judged. Contrast enhancement was assessed and the intensity (marked, moderate, mild, or no enhancement) and the local distribution were described (homogenous, inhomogenous or spongy; marginal enhancement was noted if present).

Results

CT findings

All 10 patients had localized hyperostosis of varying degrees. The sites most frequently and extensively affected were the medial portions of the sphenoid wings and orbital walls. The lateral elements of the sphenoid wings typically showed varying extensions of postoperative bone defects. The walls of the paranasal sinuses and the clinoid processes were less frequently involved, and the sellar and clival region only rarely demonstrated hyperostosis. In nine of 10 patients the hyperostotic alterations extended beyond the sutures of the sphenoid bone at at least one point. Seven of 10 patients showed markedly increased density of the hyperostotic bone, relative to the density of compact or cortical zones of the bone of the opposite side. In all patients with increased density of the hyperostotic bone there were irregular clotted plaque- and whorl-shaped structures. In two patients with spongiosalike hyperostosis the structure was trabecular and somewhat coarse; in one patient with circumscribed bone enlargement the osseous structures remained normal. In seven patients no laminar bone architecture was visible in the hyperostotic zone.

MR findings

In eight of 10 patients MR (Table 1) showed mild or moderate hyperintensity, but also in a few patients showed marked hyperintensity in areas within the CT-proved hyperostotic bone: the signals were clearly higher in these areas than in the corresponding contralateral bone (which was almost free of signal). This hyperintensity was found in T2-, proton density– and T1-weighted images. In one patient (patient 8) no difference between the signal intensity in the affected and contralateral normal bone was visible in any sequence. In the majority of the patients the structure of the hyperostotic area was inhomogenous; in nine of 10 the hyperostotic area presented without distinguishable laminar architecture.

In two patients (patients 1, 6) some areas of hyperostosis on CT showed marked or strong enhancement in MR after administration of gadopentetate dimeglumine (Fig 1). Five other patients showed moderate enhancement (Fig 2) and two other patients mild or weak enhancement in parts of the hyperostosis. The distribution of the enhancement was inhomogenous and was clearly accentuated towards the borders of the hyperostosis in some patients (patients 1, 2). The follow-up MR study in patient 1 demonstrated a clearly detectable shift in the local distribution of the enhancement; corresponding CT proved the progression of the hyperostotic mass (Fig 1).

TABLE 1: MR findings in hyperostosis

Patient	Signal Intensity of Hyperostotic Mass		Contrast Enhancement	
	T2-weighted images	Proton density-weighted images	T1-weighted images	Postcontrast T1-weighted images
1a	mild increase	mild increase	moderate increase	—
1b	moderate increase	mild increase	moderate increase	marked enhancement, inhomogenous
1c	—	—	marked increase	marked enhancement, inhomogenous, marginal accentuation
2	mild increase	marked increase	moderate increase	moderate enhancement, spongy, marginal accentuation
3	mild increase	mild increase	mild increase	moderate enhancement, spongy
4	mild increase	mild increase	moderate increase	mild enhancement, spongy
5	mild increase	mild increase	moderate increase	moderate enhancement, spongy
6	—	—	marked increase	marked enhancement, inhomogenous
7	—	—	moderate increase	moderate enhancement, inhomogenous
8	normal (free of signal)	normal (free of signal)	normal (free of signal)	not enhancing
9	mild increase	moderate increase	moderate increase	moderate enhancement
10	mild increase	mild increase	mild increase	mild enhancement

Note.—Relative signal intensity in T2-, proton density–, and T1-weighted images, and contrast enhancement of hyperostotic mass relative to contralateral normal bone.

Discussion

Some authors have postulated that the hyperostosis in sphenoid wing meningiomas may be a reactive process of the bone in the vicinity of meningiomas, perhaps promoted by nutritive effects of the well-known hyperperfusion of the tumor (7, 8). The concept of "reactive" hyperostosis has been not infrequently used in this sense in the radiologic literature (9, 10). However, many other investigators have contrarily favored a causal relationship between the meningiomatous tumor infiltration of the bone and a resulting "infiltrative" bone enlargement (3–6), a model that may include undetermined (intercellular) "reactive" factors, too.

Pathologic findings of hyperostosis have been extensively investigated in sphenoid wing meningiomas. A high incidence of histologically proved tumor infiltration was reported correspondingly in all larger series of sphenoid wing meningiomas (4–6, 11–13) and for this subgroup of meningiomas the "infiltrative" pathogenesis of hyperostosis is most favored (4–6, 13). It should be emphasized that even authors who proposed "reactive" pathogenesis of hyperostosis (7, 8) reported high incidences of meningiomatous bone infiltration (21 of 23 patients of Rowbotham [8]), but these authors merely denied that the bone mass was originating from (modified) tumor cells.

In the hyperostotic "en plaque" type of sphenoid wing meningioma the subdural tumor compartment forms only a small carpet; the mass effect on the brain and orbit is produced entirely by the massive infiltrative hyperostosis (5, 11–13). Because these tumors are frequent at this site of the cranium and extremely rare at others (11–13), it has been also proposed that there may be a primary disposition or "local factor" towards meningiomatous bone infiltration at the sphenoid wings (6, 11).

Some longitudinal studies (16–19) have shown the recurrence rate of meningiomas to be highly dependent on surgical strategy, with the best results obtained in operations including complete resection (19) of the underlying bone. Sphenoid wing meningioma has high recurrence rates (16–18) that are explained as result of the difficulty of completely or even radically resecting bone at this site (4, 5). We decided to study the MR characteristics of meningiomas, because it seems to represent one cause of meningioma recurrence. We decided to examine the highly selected group of patients with recurrent, histologically proved sphenoid wing meningiomas, because these tumors constitute a homogenous group with regard to the histopathology of hyperostosis.

A high preponderance of female patients and the (postoperative) distribution of the hyperostosis of our patients is consistent with other reports (4–6, 12). The pattern of CT findings in our patients is similar to earlier CT descriptions of local distribution in patients with sphenoid wing meningiomas (4, 10) and the CT features found in hyperostotic meningiomas en plaque (11). Thus we feel that the group studied forms a representative sample of patients with sphenoid wing meningiomas after surgical therapy and with advanced hyperostosis. Although histological

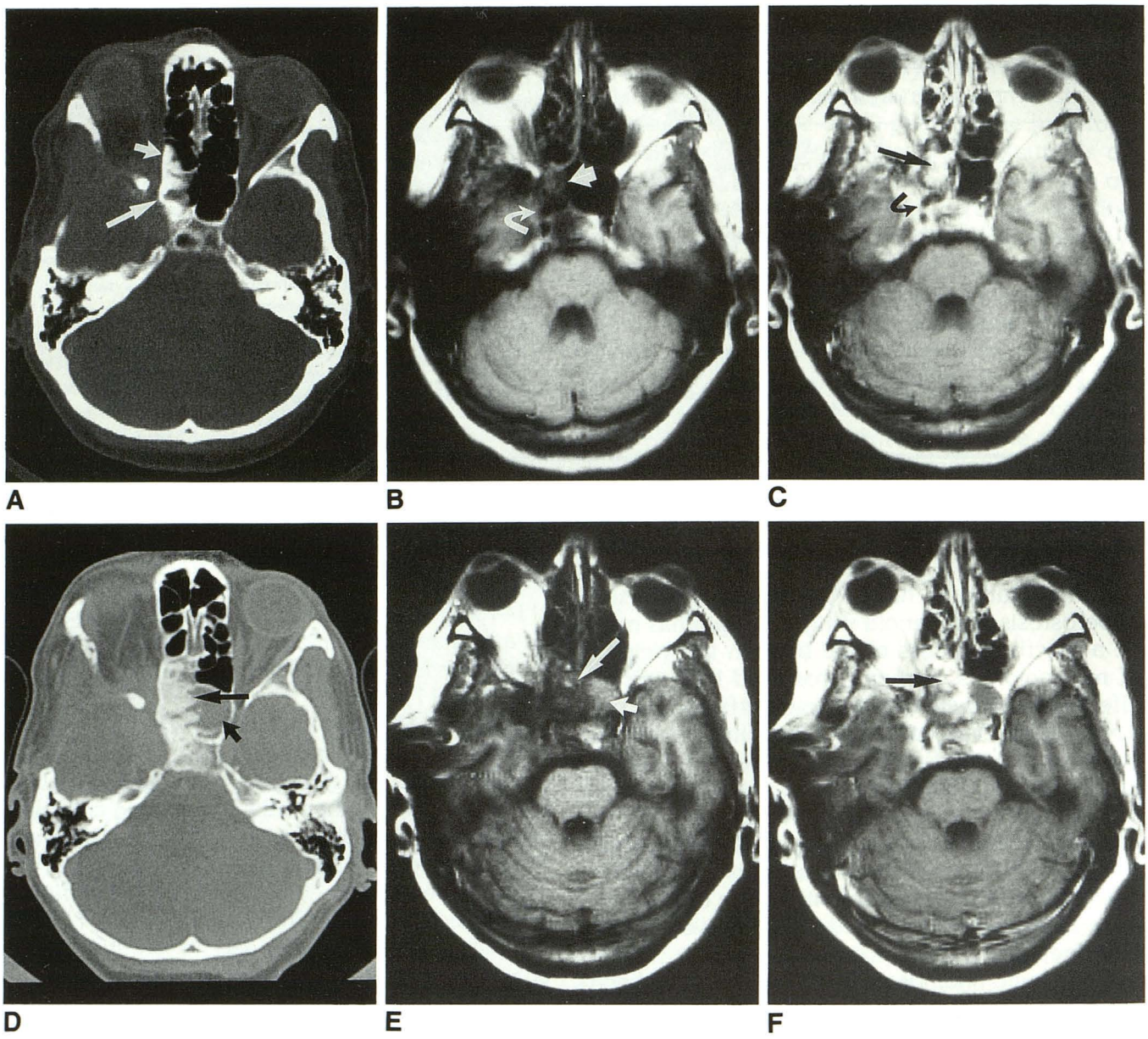

Fig. 1. *A–C*, Demonstration of gadolinium enhancement in hyperostotic mass. Patient 1, right en plaque meningioma, second study, 6 years after first operation. Right exophthalmos. Extensive areas of bone resections in orbital walls and pterional vault. Marked new bone formation in lateral walls of right sphenoidal sinus and ethmoidal cells. Axial CT and MR.

A, CT, bone window. Patchy and hyperdense structure of new bone formation in right sphenoidal sinus (*long arrow*) and ethmoidal cells (*short arrow*). *B*, T1-weighted axial image (315/14/1), moderate hyperintensity, cloudy structure in corresponding area (*straight arrow*). Carotid encasement (*curved arrow*). *C*, T1-weighted axial image (315/14/1) after 0.1 mmol Gd-DTPA/kg bodyweight shows strong and inhomogenous enhancement, pronounced at the borders of the new bone formation (*straight arrow*). Carotid encasement (*curved arrow*). Additional enhancement in sinus cavernosus.

D–F, Follow-up study with increase of mass effect. Same patient (third study), after reoperation and 2 years after second study. Progression of exophthalmus; fluid retention in left sphenoid sinus. Axial CT and MR. *D*, CT, bone window. Proliferation of the hyperostosis (*long arrow*), with higher densities and irregular caval surface. Fluid in left sphenoid sinus (*short arrow*). *E*, T1-weighted axial image (315/14/1). Inhomogenous hyperintensity of bony formation (*long arrow*). Note increased signal intensities corresponding to of fluid retention in left sphenoid sinus (*short arrow*). *F*, T1-weighted axial image (315/14/1), after administration of gadopentetate dimeglumine. Strong inhomogenous enhancement in hyperostotic formation, but with a different local distribution than in *B* and *C* (*arrow*).

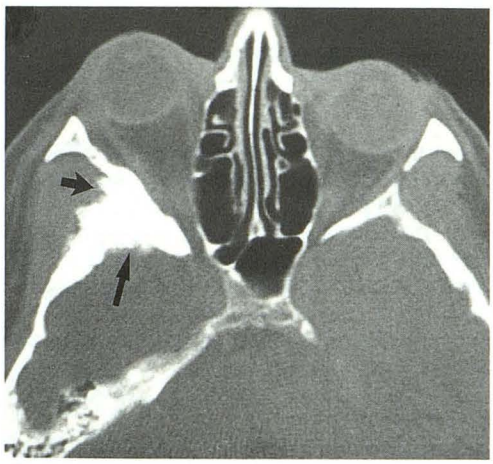

A

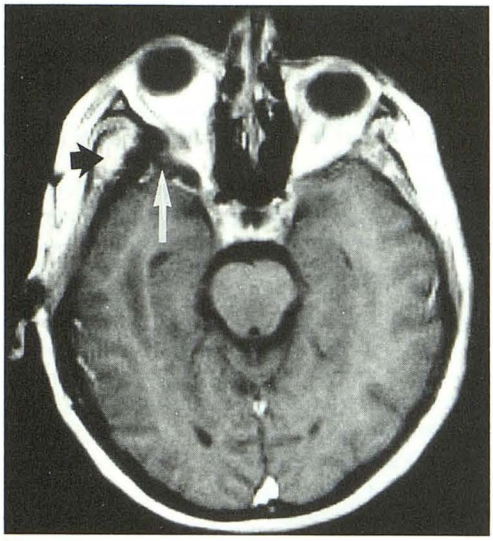

B

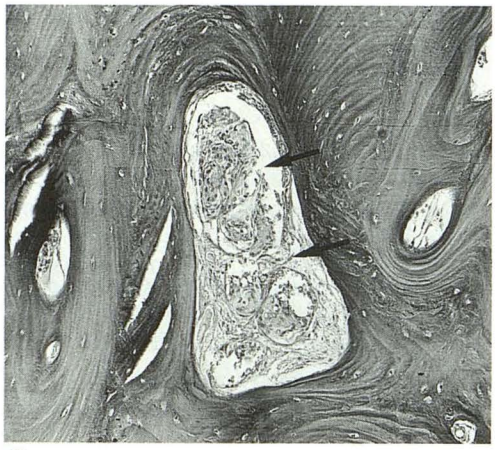

C

Fig. 2. *A–C*, Patient 3, right meningioma of en plaque type, 2 years after operation. Marked right exophthalmos.

A, CT, bone window. Marked hyperostosis (*long arrow*) at lateral orbital walls. Note spiculated external surface (*short arrow*) near extracranial meningioma mass (see *B*). *B*, T1-weighted axial image (315/14/1) after 0.1 mmol gadopentetate dimeglumine shows mild, spongiform enhancement (*white arrow*) in the medial portion of the hyperostotic bone. Homogenous enhancement of extracranial soft tissue mass (*black arrow*) over surface with spiculated appearance on CT (see *A*). *C*, Histologic specimen from involved bone in patient 3. EDTA-decalcified bone, hemotoxylin-eosin, X 82,5. The Haversian channels are filled by cones of meningiotheliomatous meningioma (*arrows*).

confirmation of meningiomatous bone infiltration was available in only four of 10 patients, this must be highly suspected in at least some other patients, based on general experience discussed above (4–6, 11, 12). Hyperostosis appeared on CT as compacta-dense, whorl-shaped, and inhomogenous structure with local disappearance of the laminar architecture of the bone. The changes in the fine structure of the bone presumably included a marked increase in the density of osseous calcification (quantitative chemical analysis not performed). These CT features resemble reported histopathologic features of irregular bone morphology (3, 7, 8) in hyperostosis but seemingly do not demonstrate correlates of the laminar growth that has been reported from histological studies, too (3, 8).

MR showed mildly or sometimes moderately increased signal intensities of the CT-proved hyperostosis, as compared with the contralateral bone. The slightly increased signal intensity in contrast-free images was seen exactly in the same areas in which CT had demonstrated high density and presumably dense calcification. This was not expected, because the effects of increased calcification alone do not explain increases in signal intensity. However, it has been found that MR signal intensities in areas of intracranial calcifications do not simply (or inversely) correlate with corresponding CT densities (20). It has been suspected that either calcium-independent soft tissue characteristics or the concentration of certain trace elements (Fe) in the calcification may influence the signal intensity in such areas (20), but the precise relations are uncertain. We can only speculate that tumor tissue in the bone and especially in the Haversian channels could have some influence on the slightly increased signal intensity in the hyperostotic tissue (Fig 2).

Inhomogenous intraosseous contrast enhancement of varying distribution and degree was seen in parts of the hyperostotic bone in most patients. In one patient the progression of hyperostosis correlated with marked alterations in the pattern of enhancement which remained accentuated at the (changing) borders. There is no physiological enhancement of osseous tissue following administration of gadopentetate dimeglumine. The massive, predominantly homogenous tumor enhancement in meningiomas is well established (15). In view of the selection of our patients the possibility of bone infiltration was believed especially high in our patients, although confirmatory histological specimens existed in only four patients. We suspect that contrast enhancement in hyperostotic bone of the sphenoid wings may be enhanced meningiomatous tumor tissue infiltrating the bone. The restriction of the enhancement

to bone segments of the hyperostotic mass subdivides areas that appear more uniform in CT scans. This leads to the assumption that certain tissue differentiations are only depicted by (contrast-enhanced) MR. There were gross changes of marginal enhancement in a follow-up MR study of a patient with enlarging bone apposition (patient 1). Some authors reported marginally arranged laminar growth in infiltrative hyperostosis (3, 7, 8) and it may be speculated that the marginal and unstationary gadolinium enhancement demonstrates imaging correlates of such laminar and marginal growth. However, prospective histopathologic confirmation is certainly required.

The possibility that contrast enhancement may be a tool in the diagnosis and evaluation of bony infiltration in meningiomas merits further considerations, because this part of the tumor is strongly implicated in recurrence. The surgical strategy (10, 12) and the decision whether to give adjuvant radiation therapy postoperatively (21) could be influenced by improved diagnostic evaluation of hyperostosis. Because MR findings in hyperostosis occurring in meningiomas at other sites, or in different tumor "stages," may differ from those presented here, hyperostosis in meningiomas requires further investigation.

References

1. Cushing H, Eisenhardt L. *Meningiomas: their classification, regional behaviour, life history and surgical results.* Springfield: Thomas, 1938
2. Gold LHA, Kieffer SA, Peterson HO. Intracranial meningiomas. A retrospective analysis of the diagnostic value of plain skull films. *Neurology* 1969;19:873–878
3. Freedman H, Forster FM. Bone formation and destruction in hyperostoses associated with meningiomas. *J Neuropathol Exp Neurol* 1948;7:69–80
4. Bonnal J, Thibaut A, Brotchi J, Born J. Invading meningiomas of the spenoid ridge. *J Neurosurg* 1980;53:587–599
5. Derome PJ, Guiot G. Bone problems in meningiomas invading the base of the skull. *Clin Neurosurg* 1978;25:435–451
6. Pompili A, Derome PJ, Visot A, Guiot G. Hyperostosing meningiomas of the sphenoid ridge. Clinical features, surgical therapy, and long-term observations: Review of 49 cases. *Surg Neurol* 1982;17:411–416
7. Kolodny A. Cranial changes associated with meningioma "dural endothelioma". *Surg Gynecol Obstet* 1929;48:231–235
8. Rowbotham GF. The hyperostosis in relation with the meningiomas. *Br J Surg* 1939;26:593–622
9. Taveras JM, Wood EH. *Diagnostic Neuroradiology.* Baltimore: William & Wilkins, 1976: Vol I, 165–167
10. Marquardt B, Voigt K. Kraniozerebrale Tumoren. In: Dihlmann W, Stender HS, eds.: *Schinz: Radiologische Diagnostik*, 7th ed. Stuttgart: Thieme, 1986:430–441
11. Kim KS, Rogers LF, Goldblatt D. CT features of hyperostosing meningiomas en plaque. *AJNR Am J Neuroradiol* 1987;8:853–859
12. Castellano F, Guidetti B, Olivecrona H. Pterional meningiomas "en plaque". *J Neurosurg* 1952;9:188–196
13. Kim KS, Rogers LF, Lee C. The dural lucent sign: Characteristic Sign of hyperostosing meningioma en plaque. *AJNR Am J Neuroradiol* 1983;4:1101–1105
14. Zimmerman RD, Fleming CA, Saint-Louis LA, Lee BC, Manning JL, Deck MD. Magnetic resonance imaging of meningiomas. *AJNR Am J Neuroradiol* 1985;6:149–157
15. Schörner W, Felix R, Claussen et al. Kernspintomographische Diagnostik von Hirntumoren mit dem Kontrastmittel Gadolinium-DTPA. *ROFO* 1984;141:511–518
16. Mirimanoff RO, Dosoretz DE, Linggood RM, Ojemann RG, Martuza RL. Meningioma: analysis of recurrence and progression following neurosurgical resection. *J Neurosurg* 1985;62:18–24
17. Adegbite A, Khan MI, Paine KW, Tan LK. The recurrence of intracranial meningiomas after surgical treatment. *J Neurosurg* 1983;58:51–56
18. Melamed S, Sahar A, Beller AJ. The recurrence of intracranial meningiomas. *Neurochirurgia* 1979;22:47–51
19. Simpson D. The recurrence of intracranial meningiomas after surgical treatment. *J Neurol Neurosurg Psychiatry* 1957;20:22–39
20. Schörner W, Kunz D, Henkes H, Sander B, Schmidt D, Felix R. Nachweis von Verkalkungen in der Magnetresonanztomographie. Einfluss verschiedener Parameter auf die MRT-Darstellung zerebraler Verkalkungen. *ROFO* 1991;154:430–437